McKenzie et al., 2018, Continental growth histories revealed by detrital zircon trace elements: A case study from India: Geology, https://doi.org/10.1130/G39973.1.

Supplementary Information

Table S1. Samples

Sample #	Region	Zone	Stratigraphic Unit	Depositional Age	GPS/Reference
DBMK1	Southern India	Kaldagi Basin	Kaldagi Gr.	Late Archean-Paleoproterozoic	15°56.157'; E075°40.594'
DBMK2	Southern India	Kaldagi Basin	Kaldagi Gr.	Late Archean-Paleoproterozoic	N15°59.938'; E074°30.349'
RA10	Central India	Aravalli-Delhi Orogenic Belt	Delwara Fm.	Paleoproterozoic	McKenzie et al., 2013
RA05	Central India	Aravalli-Delhi Orogenic Belt	Jhamarkotra Fm.	Paleoproterozoic	McKenzie et al., 2013
GH1226	Central India	Aravalli-Delhi Orogenic Belt	Jhamarkotra Fm.	Paleoproterozoic	N24°42.422'; E073°38.257'
KRSV	Central India	Vindhyan Basin-Son Valley	Kaimur Gr.	Mesoproterozoic	McKenzie et al., 2011
RVK1	Central India	Vindhyan Basin-Rajasthan	Kaimur Gr.	Mesoproterozoic	McKenzie et al., 2013
DA1	Central India	Marwar Basin	Nagaur Gr.	Early Cambrian	McKenzie et al., 2011
CRP04	Northern India	Tethyan Himalaya	Haimanta Gr.	Early Cambrian	N32°42.979'; E076°40.410'
MGM01	Northern India	Lesser Himalaya	Shimla Gr.	Cryogenian	N30°20.664'; E078°07.701'
MGT01	Northern India	Lesser Himalaya	Tal Gr.	Early-Middle Cambrian	N30°20.965'; E078°10.855'

2. U-Pb and TE LASS-ICPMS analysis

Zircon grains were selected from a bulk heavy mineral separate using standard techniques and press mounted onto an adhesive grain mount. Grains were screened using a binocular microscope for microscopic cracks and inclusions. Selected grains have c-axis dimensions between 200 μm and – 1000 μm. Following the methodology of (Kylander-Clark et al., 2013), simultaneous measurement of U-Th-Pb isotopic and trace element abundances was undertaken on the same ablation volume using Laser Ablation Split Stream (LASS) ICPMS analysis at the University of Texas. U-Th-Pb isotopic and trace element abundances were measured using two ThermoFisher® Element II HR-ICPMS' coupled to a Photon Machines® Analyte G.2 ArF 192 nm Excimer Laser. A large-volume (~30 cm^3; HeLex® cell) sample cell was used to minimize ablation volume and reduce washout time to <0.3 s, critical for obtaining <1.5 μm depth resolution. Optimal signal strengths were attained using a 50 μm spot diameter, 10 Hz repetition rate and a 6 mJ energy setpoint with 17% beam attenuation (1.67 $J.cm^{-2}$; pulse width < 4 ns). Interference from oxide masses was minimized by tuning gas flows such that UO <0.5%. Before each analysis, the grain surface was cleaned of surficial Pb by firing 6 laser shots using an 80 μm spot

diameter. For U-Th-Pb isotopic abundance measurements, correction for instrumental drift and laser-induced elemental fractionation was addressed via analysis of zircon standard GJ1 (Slama et al., 2007), using a standard-sample-bracketing routine. Accuracy of the down-hole fractionation correction was assessed by multiple analyses of secondary zircon standards Pak-1 and Plesovice (Slama et al., 2007). Average $^{207}Pb/^{206}Pb$ ages for each of the secondary standards were within acceptable limits of reported TIMS ages (Table S1). Trace element (TE) abundances were calculated by interleaving analyses of USGS basaltic glass standard GSD-1G (Jochum et al., 2005) among samples and internally-normalizing unknowns to stoichiometric SiO_2. Chondrite-normalized TE abundances were calculated using the values from (Sun and McDonough, 1989). Reduction of isotopic and elemental data was performed off-line using the Iolite package (Paton et al., 2011). Residuals to the down-hole fractionation model for zircon GJ1 were typically <1.5% of the measured average $^{206}Pb/^{238}U$ ratio, indicating predictable down-hole behavior. Ages were calculated at the 95% confidence level using Isoplot v.3 (Ludwig, 2003) and the decay constants recommended by the IUGS Subcommission in Geochronology (Steiger and Jäger, 1977). Raw U-Pb isotopic ratios and TE abundances are presented in Tables S1 and S2, respectively.

Limits of Detection (LOD) were calculated with the following formula (Longerich et al., 1996)

$$LOD = \frac{1}{S}\left[3\times 1\sigma_b \times \sqrt{\frac{1}{n_b}+\frac{1}{n_a}}\right]$$

where $1\sigma_b$ is the standard deviation of the background measurement, n_b is the number of measurements performed by the mass spectrometer during the background integration, n_a is the number of measurements performed by the mass spectrometer during the sample integration and S is the sensitivity (cps/ppm) calculated using Si in zircon as an internal standard (32.94 wt.%). LOD values averaged over three analytical sessions are: 2.68 ppm for Ti, 0.33 ppm for Y, 0.16 ppm for La, 0.04 ppm for Ce, 0.02 ppm for Pr, 0.18 ppm for Nd, 0.38 ppm for Sm, 0.14 ppm for Eu, 0.59 ppm for Gd, 0.05 ppm for Tb, 0.61 ppm for Dy, 0.06 ppm for Ho, 0.51 ppm for Er, 0.07 ppm for Tm, 0.27 ppm for Yb, 0.05 ppm for Lu, 0.44 ppm for Hf, 0.13 ppm for Ta, 0.07 ppm for Th and 0.02 ppm for U.

3. Monte-Carlo bootstrap analysis

We follow the Monte Carlo bootstrap approach detailed in Keller and Schoene (2012) to estimate average values for each of the TE abundance ratios. In order to minimize the effect of over-sampling zircon age peaks, sample weights were assigned to each zircon age in the database before bootstrap analysis. Sample weights were assumed to be inversely dependent on temporal U-Pb age density according the following relationship:

$$W_i \propto 1 \Big/ \sum_{j=1}^{n} \left(\frac{1}{\left((t_i - t_j)/a \right)^2 + 1} \right)$$

where, W_i is the weight of sample i, n is the number of grains, t is the zircon $^{207}Pb/^{206}Pb$ age and a is a normalization coefficient (40 Myr). The Monte Carlo bootstrap analysis consisted of the following steps:

1. A subset of zircon grains was resampled according to sample weights.
2. Synthetic data points were drawn from Gaussian distributions around the mean of each of the resampled data points.
3. The synthetic data were sorted into 250 Myr bins and means and variance were calculated for each TE abundance ratio.
4. Steps 1-3 were repeated 10,000 times.
5. A total mean and standard error of the mean was calculated for each bin.

Bootstrap analysis was performed using MATLAB code written by the authors. Random number generation for steps 1 and 2 were generated using the Mersenne Twister pseudorandom number generator implemented by MATLAB.

Fig. S1: Raw zircon U-Pb age and TE data

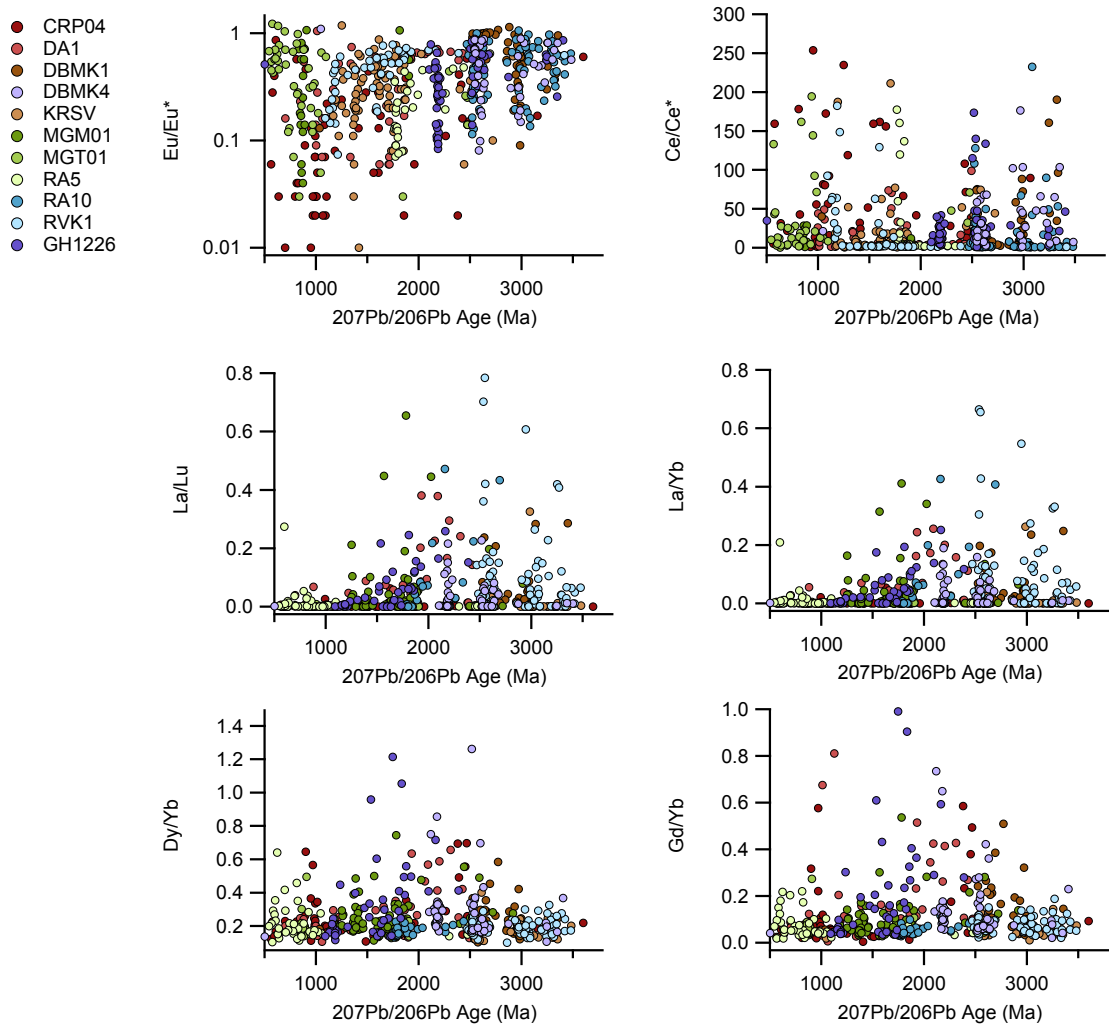

Table S1. Zircon U-Pb age data (data repository).

Table S2. Zircon trace element data (data repository).

REFERENCES

Jochum, K. P., Willbold, M., Raczek, I., Stoll, B., and Herwig, K., 2005, Chemical Characterisation of the USGS Reference Glasses GSA-1G, GSC-1G, GSD-1G, GSE-1G, BCR-2G, BHVO-2G and BIR-1G Using EPMA, ID-TIMS, ID-ICP-MS and LA-ICP-MS: Geostandards and Geoanalytical Research, v. 29, no. 3, p. 285-302.

Keller, C. B., and Schoene, B., 2012, Statistical geochemistry reveals disruption in secular lithospheric evolution about 2.5 Gyr ago: Nature, v. 485, no. 7399, p. 490-U100.

Kylander-Clark, A. R. C., Hacker, B. R., and Cottle, J. M., 2013, Laser-ablation split-stream ICP petrochronology: Chemical Geology, v. 345, p. 99-112.

Longerich, H. P., Jackson, S. E., and Gunther, D., 1996, Laser ablation inductively coupled plasma mass spectrometric transient signal data acquisition and analyte concentration calculation: Journal of Analytical Atomic Spectrometry, v. 11, no. 9, p. 899-904.

Ludwig, K. R., 2003, Isoplot 3.0 – a geochronological toolkit for Microsoft excel: Berkeley Geochronology Center, Berkeley, Special Publication, v. 4.

Paton, C., Hellstrom, J., Paul, B., Woodhead, J., and Hergt, J., 2011, Iolite: Freeware for the visualisation and processing of mass spectrometric data: Journal of Analytical Atomic Spectrometry, v. 26, p. 2508-2518.

Slama, J., Kosler, J., Crowley, J. L., Gerdes, A., Hanchar, J., Horstwood, M., Morris, G. A., Nasdala, L., Norberg, N., Schaltegger, U., Tubrett, M. N., and Whitehouse, M. J., 2007, Plesovice zircon - A new natural standard for U-Pb and Hf isotopic microanalysis: Geochimica Et Cosmochimica Acta, v. 71, no. 15, p. A947-A947.

Steiger, R. H., and Jäger, E., 1977, Subcommission on geochronology; Convention on the use of decay constants in geo- and cosmochronology: Earth and Planetary Science Letters, v. 36, p. 359-362.

Sun, S.-s., and McDonough, W. F., 1989, Chemical and isotopic systematics of oceanic basalts: implications for mantle composition and processes: Geological Society, London, Special Publications, v. 42, p. 313-345.